Toxicity from radiation therapy associated with abnormal transcriptional responses to DNA damage

Kerri E. Rieger*†, Wan-Jen Hong*†, Virginia Goss Tusher*, Jean Tang*, Robert Tibshirani‡, and Gilbert Chu*§

*Departments of Medicine and Biochemistry, and ‡Health Research and Policy, and Statistics, Stanford University School of Medicine, Stanford, CA 94305

Edited by Patrick O. Brown, Stanford University School of Medicine, Stanford, CA, and approved March 14, 2004 (received for review November 22, 2003)

Toxicity from radiation therapy is a grave problem for cancer patients. We hypothesized that some cases of toxicity are associated with abnormal transcriptional responses to radiation. We used microarrays to measure responses to ionizing and UV radiation in lymphoblastoid cells derived from 14 patients with acute radiation toxicity. The analysis used heterogeneity-associated transformation of the data to account for a clinical outcome arising from more than one underlying cause. To compute the risk of toxicity for each patient, we applied nearest shrunken centroids, a method that identifies and cross-validates predictive genes. Transcriptional responses in 24 genes predicted radiation toxicity in 9 of 14 patients with no false positives among 43 controls ($P = 2.2 \times 10^{-7}$). The responses of these nine patients displayed significant heterogeneity. Of the five patients with toxicity and normal responses, two were treated with protocols that proved to be highly toxic. These results may enable physicians to predict toxicity and tailor treatment for individual patients.

Ionizing radiation (IR) is used to treat ≈60% of cancer patients (1). Although most patients tolerate treatment, 5–10% of patients suffer significant toxicity. Risk factors include age, concurrent chemotherapy, and anatomical variations from factors such as congenital malformations, postsurgical adhesions, fat content, and tissue oxygenation (1), or concurrent illnesses such as diabetes and autoimmune diseases such as lupus (2–4). These factors account for an unknown fraction of adverse radiation reactions.

In rare cases, radiation sensitivity can be attributed to specific genetic mutations. Diseases of IR sensitivity include ataxia telangiectasia (AT) (5), AT-like disorder (6), Nijmegen breakage syndrome (7), and radiosensitivity with severe combined immunodeficiency (8), but these autosomal recessive diseases are uncommon. Heterozygosity for mutations in ATM, the gene mutated in AT, may occur in 1% of individuals and has been reported to confer moderate sensitivity to IR in tissue culture (9). However, relatively few adverse radiation reactions are associated with ATM mutations (10–12).

Several attempts have been made to correlate radiation toxicity with cellular responses to IR *ex vivo*. Cultured skin fibroblasts from patients with acute radiation toxicity showed decreased survival after IR in some studies (13) but not others (14, 15). Lymphocytes from patients with radiation toxicity showed a paradoxical decrease in IR-induced apoptosis (16). Lymphocytes from breast cancer patients with severe skin reactions developed abnormal numbers of chromosome aberrations after IR exposure (17). However, there was a large overlap between radiation-sensitive patients and controls in these assays. To determine whether *ex vivo* responses to IR might lead to a useful clinical test, we hypothesized that cells from patients with radiation toxicity have abnormal transcriptional responses to DNA damage.

Methods

Radiation-Sensitive Patients and Controls. A total of 57 subjects were enrolled between 1997 and 2002 with informed consent in accordance with Stanford University regulations for human subjects research. Fourteen radiation-therapy patients suffered unusual levels of radiation toxicity within 1 month of treatment, as judged by their radiation oncologist (Table 1). Peripheral blood was obtained at least 2 months after completion of treatment and resolution of any toxicity. The grade of toxicity was scored according to the Radiation Therapy Oncology Group acute radiation morbidity scoring criteria (www.rtog.org/members/toxicity/main.html). In 11 of the 14 patients, toxicity was severe enough to require interruption or early termination of treatment, which helped limit the reported toxicities to grades 2 and 3. Ethnic origins of the radiation-sensitive patients were European (11), Hispanic (1), East Asian (1), and South Asian (1), and their average age was 51 years.

Thirteen patients with toxicity limited to grades 0 or 1 were enrolled as controls. We attempted to match this control group to the radiation-sensitive patients by radiation field and dose, tumor type, gender, and concurrent chemotherapy (Table 1 and Table 2, which is published as supporting information on the PNAS web site). The study incorporated significant heterogeneity in tumors and treatment sites. Matching the radiation-sensitive and radiation control groups facilitated our goal to find gene responses that predicted acute toxicity regardless of tumor diagnosis or treatment site. Ethnic origins of the radiation control patients were European (11), African American (1), and Indonesian (1), and their average age was 59 years. Because the risk of radiation toxicity increases with age (18), the older age of the radiation control patients should enhance the validity of our results.

Fifteen patients diagnosed with skin cancer before age 40 were additional controls. We planned to expose the cells to UV radiation as well as IR to explore the possibility that some radiation-sensitive patients might have defects in responding to more than one type of DNA damage. Because skin cancer is associated with UV radiation exposure, skin cancer patients were included as controls to ensure that they would not be assigned a high risk for radiation toxicity. Ethnic origins of the skin cancer patients were European (14) and Hispanic (1), and their average age was 38 years.

Fifteen healthy subjects without any history of cancer were matched to the skin cancer patients, providing a third group of controls. Ethnic origins of the healthy subjects were European (14) and Hispanic (1), and their average age was 31 years.

Cell Lines and Treatment with UV Radiation and IR. Lymphoblastoid cell lines were established by immortalization of B lymphocytes with Epstein–Barr virus from the B95-8 monkey cell line, grown in RPMI medium 1640 (GIBCO) with 15% heat-inactivated FBS/1% penicillin/streptomycin/2 mM glutamine and stored in liquid nitrogen. We chose to use lymphoblastoid cell lines

This paper was submitted directly (Track II) to the PNAS office.

Abbreviations: IR, ionizing radiation; AT, ataxia telangiectasia; ATM, AT mutated; NSC, nearest shrunken centroids; HAT, heterogeneity-associated transformation.

†K.E.R. and W.-J.H. contributed equally to this work.

§To whom correspondence should be addressed at: Division of Oncology, CCSR 1145, Stanford University Medical Center, Stanford, CA 94305-5151. E-mail: chu@stanford.edu.

© 2004 by The National Academy of Sciences of the USA

MEDICAL SCIENCES

Downloaded by guest on February 24, 2022

Table 1. Clinical characteristics of radiation-sensitive patients

Age, years	Gender	Diagnosis	Patient	Reaction	Grade	Radiation/concurrent chemotherapy
37	F	Breast cancer	RadS4*	Skin	3†	45 Gy breast
49	F	Breast cancer	RadS14	Skin	2†	50 Gy breast, 10 Gy boost/cytoxan, 5FU
53	F	Breast cancer	RadS12	Skin	2†	55 Gy breast
65	F	Breast cancer	RadS1*	Skin	3†	45 Gy breast
37	F	Hodgkin's disease	RadS10	Skin	3†	40 Gy mantle field, 10 Gy neck boost
50	M	Hodgkin's disease	RadS6	Skin	3	44 Gy mantle field
67	M	Hodgkin's disease	RadS8	Pneumonitis	2†	43 Gy mantle field, 36 Gy spade field
57	M	Low-grade lymphoma	RadS7	Mucositis	3†	50 Gy mandible & neck, 45 Gy hip
60	M	Low-grade lymphoma	RadS2*	Skin	3‡	31 Gy lacrimal glands in both orbits
41	M	Cancer of tongue	RadS3*	Mucositis	3†	70 Gy tongue/tpz, cisplatin, 5-FU
45	M	Salivary gland cancer	RadS9	Skin, mucositis	3†	40 Gy mouth, 12 Gy tongue, 48 Gy neck/cisplatin, 5FU
67	F	Endometrial cancer	RadS13	Diarrhea	3‡	42 Gy pelvis
52	F	Orbital pseudotumor	RadS11	Orbital edema	2	31 Gy orbit
33	F	Brainstem AVM	RadS5*	Brain edema	3	18 Gy stereotactic brainstem radiation

RadS6, RadS7, and RadS10 also suffered from delayed radiation reactions consisting of stroke 8 years later, osteonecrosis of the hip and jaw plus cystitis 10 years later, and breast cancer 20 years later, respectively. Patients are numbered in the order in which they appear in Figs. 1 and 3 from left to right. AVM, arteriovenous malformation; 5FU, 5-fluorouracil; tpz, tirapazamine.

*Misclassified patient.

†Interruption of treatment helped limit grade of toxicity.

‡Early termination of treatment helped limit grade of toxicity.

because they provided a renewable resource and could be compared with existing lymphoblastoid cell lines with defined mutations. Cells were subjected to mock, UV radiation, or IR treatment. For UV radiation treatment, cells were suspended at 6×10^5 cells per ml in PBS to ensure uniform exposure to UV radiation. Cells subjected to mock and IR treatment were also suspended in PBS during this period to ensure similar treatment. For UV radiation treatment, cells were exposed to 10 J/m^2 and harvested for RNA 24 h later. For IR treatment, cells were exposed to 5 Gy IR 20 h after the PBS wash and harvested for RNA 4 h later.

Microarray Analysis. Total RNA was labeled with biotin and hybridized to a U95A_v2 GeneChip microarray according to manufacturer protocols (Affymetrix, Santa Clara, CA). To account for differences in hybridization between different chips, data from hybridizations were scaled to the average of all data sets as described (19).

The data were analyzed in the form of differences in expression before and after exposure to IR or UV radiation. To identify IR- and UV radiation-responsive genes, we used the paired data option in SAM (Significance Analysis of Microarrays; available at www-stat.stanford.edu/~tibs/SAM), which ranks genes by change in expression relative to the standard deviation in multiple samples (19).

To assign risk for radiation toxicity, we used the method of nearest shrunken centroids (NSC) (20). (Software is available at www-stat.stanford.edu/~tibs/PAM.) The centroid for a class of samples is defined as a multicomponent vector in which each component is the expression of a predictive gene averaged over the samples in that class. NSC eliminates noninformative genes by shrinking the class centroids toward the overall centroid after normalizing by the within-class standard deviation for each gene. The probability for radiation toxicity associated with an expression profile was computed from its distances to the radiation toxicity and radiation control centroids. The accuracy of supervised classifiers such as NSC must be tested by cross-validation on samples not used for training (21). NSC utilizes N-fold cross-validation, in which the full set of samples is divided into N test sets. Here, we used 14 test sets ($n = 14$) in which each test set contained one radiation-sensitive patient and two or three control subjects. One test set was withheld, and the remaining samples were used to identify the classifying genes. Each sample from the test set was then classified by its nearest centroid. The procedure was repeated for each test set until every sample was classified.

Results

Analysis by SAM and NSC. To identify genes normally induced or repressed by IR or UV radiation, we applied SAM (19) to data from 9 of the 15 normal subjects. SAM identified 1,491 IR-responsive genes and 2,114 UV radiation-responsive genes, with a false discovery rate of 10% (Tables 3–6, which are published as supporting information on the PNAS web site). We previously developed NSC, which successfully identified small sets of highly predictive genes for other classification problems (20). To find predictive genes, we applied NSC to the patient samples, restricting the analysis to the IR- and UV radiation-responsive genes. To avoid selection bias, the nine normal subjects used for identifying the IR- and UV radiation-responsive genes were used in NSC for testing but not for training. The remaining 48 samples were used for both training and testing. Disappointingly, classification required 1,831 genes while generating 10 errors.

Heterogeneity-Associated Transformation. A new approach was needed to identify predictive genes. We reasoned that radiation toxicity might arise from several different underlying defects, generating divergent transcriptional responses. For example, one subset of radiation-sensitive patients could have a defect in signaling through ATM, leading to a failure to activate p53 after IR and a blunted response in p53-induced genes. Another subset could have a defect in DNA repair, leading to prolonged activation of ATM and enhanced transcription of p53-induced genes.

To address the problem of heterogeneity, we performed the following heterogeneity-associated transformation (HAT)

$$x'(i) = [x(i) - \bar{x}_c(i)]^2, \quad [1]$$

where $x(i)$ is the change in expression for gene i, and $\bar{x}_c(i)$ is the average change in expression for gene i among the control samples. HAT generates similar values from changes in gene expression that are blunted in some cases or enhanced in others and hence can capture heterogeneous abnormalities among the radiation-sensitive patients. Simulations of microarray data demonstrated that NSC/HAT is more efficient than NSC alone

Downloaded by guest on February 24, 2022

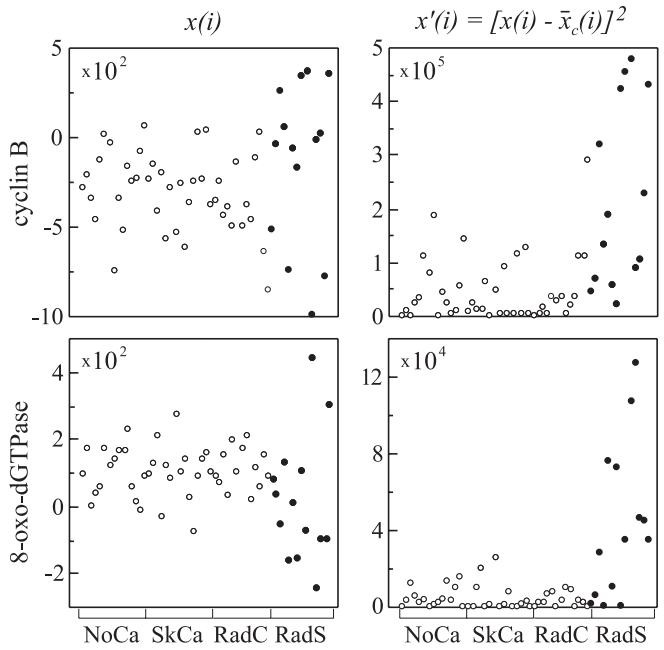

Fig. 1. Effect of HAT on gene expression data. Data are shown for 15 healthy subjects with no cancer (NoCa), 15 patients with skin cancer (SkCa), 13 control patients who received radiation without toxicity (RadC), and 14 cancer patients with radiation sensitivity (RadS). (*Left*) Shown are data for two predictive genes, cyclin B and 8-oxo-dGTPase, as changes in gene expression after DNA damage, $x(i)$, for gene i. (*Right*) How the radiation-sensitive patients are separated from the three control groups after transformation by HAT. Expression is in units provided by the Affymetrix GeneChip MICROARRAY ANALYSIS SUITE 4.0 software. Patient samples were arranged by predicted probability for radiation toxicity (see Fig. 3).

in identifying genes with heterogeneous responses but less efficient in identifying genes with homogeneous responses (22).

Genes with heterogeneous transcriptional responses were successfully identified after transforming the data with HAT. Fig. 1 shows the effect of HAT on two predictive genes, cyclin B and 8-oxo-dGTPase. When $x'(i)$ replaced $x(i)$ in NSC for the set of 1,491 IR-responsive genes and 2,114 UV radiation-responsive genes, we predicted radiation toxicity with only five errors over a wide range of values for the number of predictive genes (Fig. 2). Indeed, the 25 top-ranked probe sets (corresponding to 24 genes) predicted toxicity with five false negatives and no false positives. These classification errors were obtained by 14-fold cross-validation as described in *Methods*. Similar results were obtained when the right-hand side of Eq. **1** equaled the absolute value of the difference rather than the squared difference (data not shown). Thus, HAT enhanced the power of NSC, suggesting that the radiation-sensitive patients constitute a heterogeneous group.

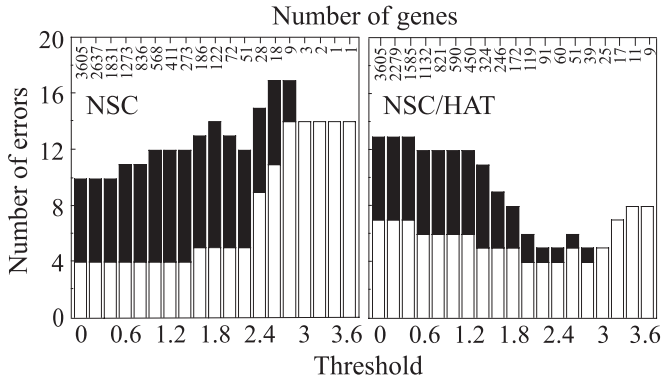

Fig. 2. Effect of HAT on predictive power. The NSC classifier was applied to 1,491 IR-responsive genes and 2,114 UV-responsive genes identified by SAM. In the NSC method, the threshold parameter determines the number of genes used for prediction (shown above the bar graphs). (*Left* and *Right*) Number of errors without and with HAT, respectively. White bars indicate the number of false negatives, and black bars indicate the number of false positives.

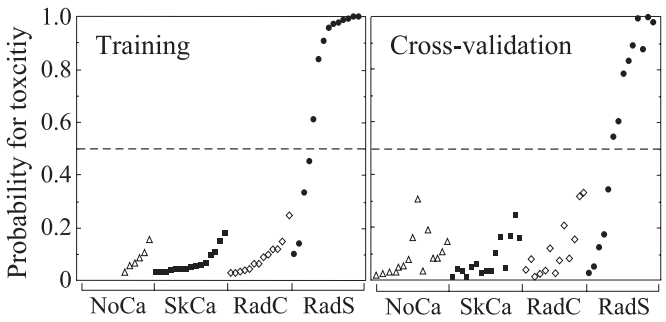

Fig. 3. Predicting radiation toxicity from transcriptional responses to IR and UV radiation. NSC/HAT identified 24 predictive genes represented by 25 probe sets. IR and UV radiation responses were used to compute the probability of toxicity for each subject. The dotted lines indicate probability of 0.5, the prospectively defined cutoff for predicting radiation toxicity. (*Left*) Probabilities for radiation toxicity calculated from the full 48-sample training set. To avoid selection bias (21), nine subjects with no cancer (NoCa) were excluded from the training set because they were used to identify the IR- and UV radiation-responsive genes. (*Right*) Probabilities calculated from 14-fold cross-validation. The nine subjects with no cancer that we excluded from the training sets were included in the test sets. SkCa, patients with skin cancer; RadC, control patients who received radiation without toxicity; RadS, cancer patients with radiation sensitivity.

Prediction of Radiation Toxicity. Of the 24 predictive genes, 20 were IR-responsive and 4 were UV radiation-responsive. From these responses, NSC/HAT computed a probability of radiation toxicity for each subject in the 48-sample training set (Fig. 3 *Left*). The separation between the radiation-sensitive patients and controls indicated a strong correlation between the responses of the 24 genes and radiation toxicity. This correlation was confirmed by 14-fold cross-validation. Each of 14 test sets was used to validate the 25 top-ranked probe sets obtained from the remaining samples. When the results of all the test sets were pooled, we predicted radiation toxicity in 9 of 14 patients (Fig. 3 *Right*). Significantly, there were no false positives among 43 controls, including the 34 controls used for NSC and the 9 control subjects used to identify the damage-response genes. The probability that such a result could have occurred by chance was $P = 2.2 \times 10^{-7}$ by Fisher's two-tailed exact test.

The genes identified during cross-validation were very similar to the genes identified from the full 48-sample training set. Among the genes identified for each of the 14 cross-validation trials, 80% were among the 24 top-ranked genes from the 48-sample training set, and 99% were among the 52 top-ranked genes from that set (Fig. 4). To test the stability of the cross-validation protocol, we performed 10 new trials of 14-fold cross-validation by withholding different subsets of patients. All 10 trials successfully predicted toxicity in the same 9 of 14 patients, with no false positives among the controls.

Delayed toxicity in the form of progressive damage after completion of treatment is a grave problem. Three patients (RadS6, RadS7, and RadS10) suffered grade 4 delayed toxicity, and all were predicted successfully (Table 1). Toxicity from extrinsic factors cannot be predicted by our approach. Of the five patients with radiation toxicity not predicted by NSC/HAT, at least two (RadS3 and RadS5) were at high risk for toxicity from

Downloaded by guest on February 24, 2022

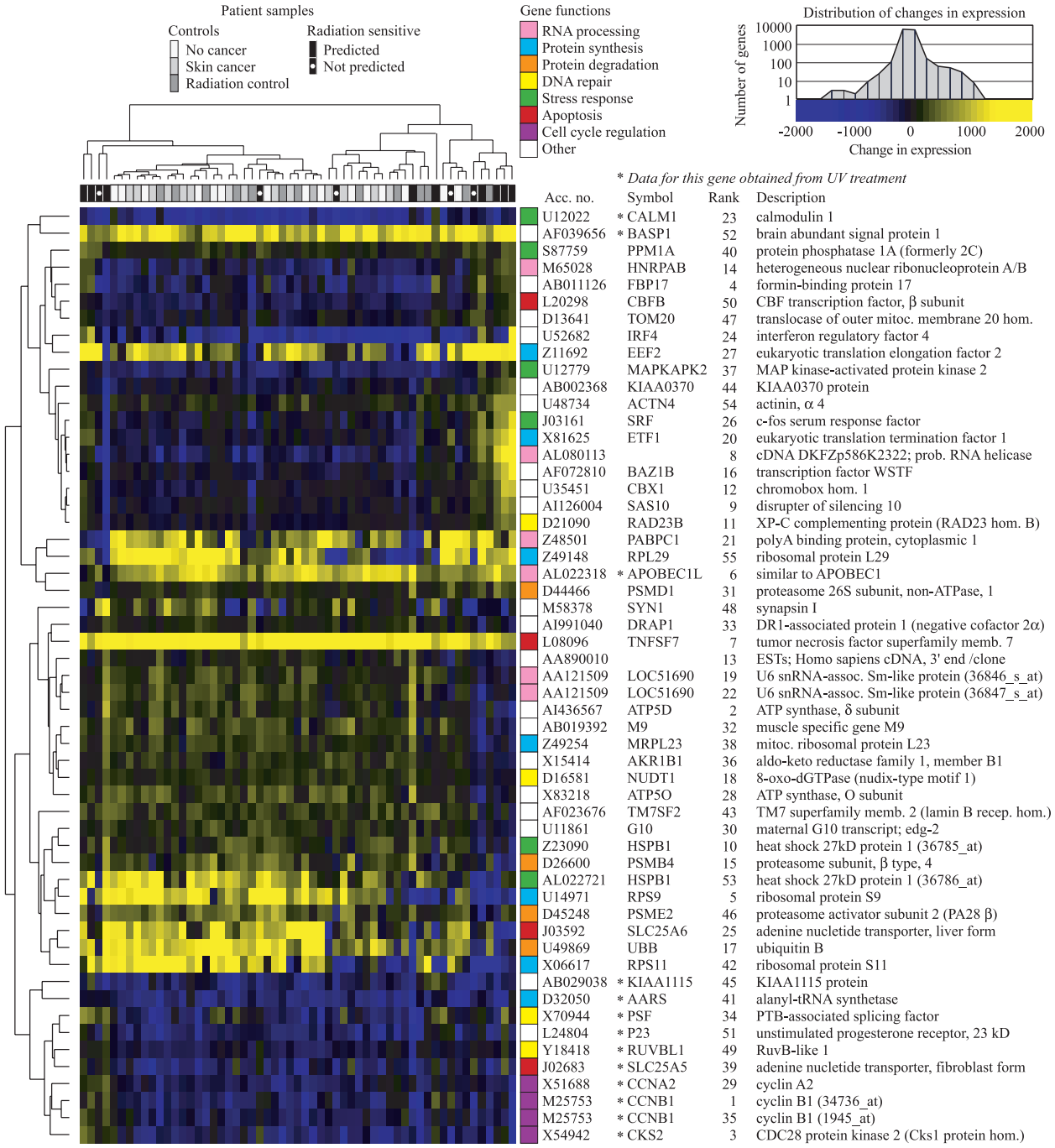

Fig. 4. Hierarchical clustering of genes predictive for radiation toxicity. Data are shown for the 52 top-ranked genes identified by NSC/HAT. Clustering used centered Pearson correlation and complete linkage and was displayed with TREEVIEW (http://rana.lbl.gov/EisenSoftware.htm). Because we used centered Pearson correlation, genes with changes in expression that varied in the same way across samples clustered together independently of average changes in expression. For example, the first two genes, *CALM1* and *BASP1*, were clustered together even though *CALM1* was generally repressed and *BASP1* was generally induced. The dendrogram above the heat map shows clustering of the 57 subjects. The dendrogram to the left of the heat map shows clustering of the 52 genes represented by 55 probe sets. The colored boxes to the right of the heat map indicate biological function of the genes. The data are for IR responses except where marked by an asterisk. GenBank accession number, symbol, and rank in our prediction protocol are listed for each gene. (*Upper Right*) Color scale and distribution of IR responses for all 12,625 probe sets. The distribution of UV radiation responses was similar (data not shown).

unconventional treatment protocols. Patient RadS3 suffered grade 3 mucositis in an experimental trial that included high-dose radiation plus tirapazamine, cisplatin, and 5-fluorouracil. Review of patient data after closure of this trial revealed that 28 of 62 (45%) suffered mucositis of grade 3 or higher. Patient RadS5 had an arteriovenous malformation that was treated with stereotactic guidance of a single 18-Gy dose to a 1.8-cm^3 volume in the midbrain and pons. After this patient was enrolled for study, Flickinger *et al.* (23) estimated that stereotactic radiotherapy to this region carries a 40–45% risk for permanent injury at the dose and volume delivered to RadS5. To determine whether RadS3 and RadS5 had an effect on the results, we excluded them and repeated the analysis. Despite the decreased number of samples available for training, NSC/HAT success-

Downloaded by guest on February 24, 2022

fully predicted toxicity in 9 of the remaining 12 cases, with no false positives among the 43 controls.

Ruling Out Confounding Variables. Because of the enormous number of genes analyzed by microarrays, transcriptional responses that seem to be predictive might instead be caused by a confounding variable. The confounding variable could be some other difference between the radiation-sensitive patients and the control subjects. For example, the 15 skin cancer patients and 15 normal subjects were younger. They were free of cancers of the internal organs, which might be associated with an abnormal response to DNA-damaging agents. Furthermore, they were never treated with IR, and some could be at risk for toxicity. To address these issues, we omitted these 30 subjects and reanalyzed the 27 radiation-therapy patients. This restricted analysis was successful despite the fewer samples available for training. A set of 13 genes yielded the same five false negatives reported above, with no false positives among the 13 controls. When tested on the 30 omitted subjects, these 13 genes predicted only three positives, consistent with the expected low risk for toxicity in the general population. The predictive genes were affected only mildly by the restricted analysis. Nine of the 13 genes were among the 24 top-ranked genes identified with the 48-sample training set, and 20 of the 24 predictive genes from the 48-sample training set were among the 81 top-ranked genes in the restricted analysis.

Heterogeneity Among the Radiation-Sensitive Patients. The 57 subjects and 52 top-ranked predictive genes identified by NSC/HAT were organized by hierarchical clustering (24). The 52 genes were obtained from the 48-sample training set and included 40 IR-responsive genes and 12 UV radiation-responsive genes (Fig. 4). The radiation-sensitive patients did not form a single cluster, suggesting that adverse reactions arise from more than one type of underlying defect. Four radiation-sensitive patients clustered loosely on the left side of the heat map. Cells from these patients had abnormal responses in many of the 52 genes, including the cluster of 9 UV radiation-responsive genes at the bottom of the heat map. These patients may have a general defect in responding to DNA damage. Five radiation-sensitive patients clustered on the right side of the heat map. These patients had a relatively normal response in the UV radiation-response gene cluster but had prominent defects in IR-response genes.

Genes with Transcriptional Responses That Predict Radiation Toxicity. No single gene predicted radiation toxicity. Instead, the response of several genes provided a signature for toxicity. The 52 top-ranked predictive genes are involved in several different cellular processes.

Four genes had roles in DNA repair. Abnormal IR responses were observed for 8-oxo-dGTPase (*NUDT1*) and xeroderma pigmentosum group C-complementing gene (*RAD23B*). The 8-oxo-GTPase hydrolyzes the oxidized nucleotide 8-oxo-dGTP to 8-oxo-dGMP, preventing misincorporation of 8-oxo-dGTP into DNA. The 8-oxo-GMP is converted to 8-oxo-dG, which has been reported to be a urinary biomarker for oxidative DNA damage (25–27) that correlates inversely with acute radiosensitivity in breast cancer patients (28). *RAD23B* targets UV radiation-induced lesions for nucleotide excision repair but may have a previously unrecognized role in repairing IR-induced base damage. Abnormal UV radiation responses were observed for genes encoding RuvB-like protein 1 (RUVBL1) and polypyrimidine tract binding protein (PTB)-associated splicing factor (PSF). Both genes may have roles in homologous recombination. RUVBL1 is homologous to bacterial RuvB, a DNA helicase that catalyses branch migration of Holliday junctions (29), and PSF promotes D-loop formation *in vitro* (30).

Five predictive genes are involved in the general stress response. Abnormal IR responses occurred in genes encoding c-*fos*, mitogen-activated protein kinase-activated protein kinase 2 (MAPKAP2) (31), heat-shock protein 27 (HSPB1), which is a substrate of MAPKAP2 phosphorylation, and protein phosphatase 1A (PPM1A), which inhibits stress-activated protein kinase cascades (32). Abnormal UV radiation responses were observed for calmodulin (CALM1) (33).

Four predictive genes are involved in the ubiquitin/proteasome protein degradation pathway (34), which is induced by oxidative stress (35). Abnormal IR responses were observed for ubiquitin B (UBB), proteasome activator subunit (PSME2), and two subunits of the 26S proteasome, β subunit 4 (PSMB4) and the non-ATPase subunit 1 (PSMD1).

Abnormal UV radiation responses occurred in three cell cycle genes: cyclin B1 (CCNB1), cyclin A2 (CCNA2) (36), and CDC28 protein kinase 2 (CKS2), which negatively regulates cyclin-dependent kinase–cyclin complexes.

Apoptosis genes included tumor necrosis factor (TNFSF7), core-binding factor (CBFB) (37), and the mitochondrial adenine nucleotide transporter (ANT). ANT regulates mitochondrial membrane permeability during apoptosis (38, 39). The fibroblast isoform of ANT (SLC25A6) responded abnormally to IR, and the liver isoform (SLC25A5) responded abnormally to UV radiation. Four predictive genes were involved in RNA processing, and the remaining 18 predictive genes were involved in a diverse set of pathways. Many well known damage-response genes such as p21 did not emerge from this analysis because they were not predictive.

Discussion

We have shown that many cases of radiation toxicity are associated with abnormal transcriptional responses to DNA damage. Classification by NSC after applying HAT predicted 9 of 14 cases of radiation toxicity with no false positives among 43 controls. Notably, the false-positive rate was very low, yielding a 95% confidence interval of 0–7%. Toxicity was predicted successfully in 64% of the radiation-sensitive patients with a 95% confidence interval of 42–87% by the exact binomial distribution. Even the lower limit of this confidence interval suggests that a significant number of adverse radiation reactions are associated with abnormal transcriptional responses. Furthermore, two of the five patients not predicted by NSC/HAT were at high risk for radiation toxicity from their treatment protocols and may have been classified properly as having normal transcriptional responses.

Our results are likely to be valid for several reasons. First, our results were subjected to cross-validation, which guards against identification of genes that later fail when tested on an independent set of samples. Our use of 14-fold cross-validation is more robust than the commonly used "leave-one-out" approach (20, 21). Second, we ruled out confounding variables by restricting analysis to the 27 radiation-therapy patients and attaining the same degree of success. Third, we successfully applied nearest centroids with HAT to the IR responses of all 12,625 probe sets on the microarray. On cross-validation, we predicted 8 of 14 cases of radiation toxicity (RadS5, RadS7, and RadS9–14) with only two false positives (RadC8 and RadC9) among the 43 controls. Thus, our results were not an artifact of gene-selection bias (21).

Finally, our protocol for predicting radiation toxicity used a plausible biological endpoint, the transcriptional response to DNA damage. Appropriately, 20 of the 24 top-ranked genes contributed IR responses, and only 4 genes contributed UV radiation responses. When we attempted to predict radiation toxicity from the less plausible endpoint of basal gene expression, we obtained a low error rate after cross-validation. However, basal expression failed our additional test of restricting analysis to the radiation-therapy patients; the prediction error rate increased significantly, and the set of predictive genes

Downloaded by guest on February 24, 2022

changed markedly (data not shown), indicating the presence of confounding variables that affected basal gene expression.

The radiation-sensitive patients seem to be heterogeneous. Some had abnormal transcriptional responses to both UV radiation and IR, and others had abnormal responses only to IR. The predictive genes may not be mutated but instead respond abnormally due to mutation of some other gene. Radiation toxicity also may arise from the combined effect of polymorphisms in several genes. A limitation of this study is that it did not identify the genetic basis for toxicity in the patients.

A second limitation is that we failed to predict toxicity in subjects with defined genetic defects. The 24 predictive genes were unsuccessful when tested on lymphoblastoid cell lines from subjects with Nijmegen breakage syndrome and AT (data not shown). Specific tests will be required to predict toxicity in these rare and unusually sensitive patients.

Finally, before a useful clinical test for radiation toxicity can be developed, our results must be confirmed with an independent cohort of patients. The low false-positive rate must be maintained so that most patients continue to receive appropriate radiotherapy. A practical test must use primary peripheral blood lymphocytes to avoid the delay associated with making lymphoblastoid cell lines. For patients with a high risk for toxicity, radiation could be administered at lower doses or waived in favor of surgery or chemotherapy.

We are indebted to the patients who generously donated blood for this study. U. Lee assisted in recruiting patients; S. Donaldson, I. Gibbs, D. Goffinet, S. Hancock, R. Hoppe, D. Kapp, S. Knox, and Q. Le referred patients from the Department of Radiation Oncology; H. Gladstone, Y. Kim, A. Lane, K. Nishimura, and J. Starr referred patients from the Department of Dermatology; M. Stonich and S. Fodor assisted with the Affymetrix GeneChip probe arrays; T. Hastie and B. Narasimhan assisted with software; and J. Budman, L. DeFazio, B. Ekstrand, S. Kim, A. Koong, and T. Tan read the manuscript. This work was supported by funding from the Medical Scientist Training Program (to K.E.R. and J.T.), a Stanford Genome training grant (to V.G.T.), a Burroughs-Wellcome Clinical Scientist Award for Translational Research (to G.C.), and National Institutes of Health Small Business Technology Transfer Grant CA75675 (to G.C. and Affymetrix).

1. Perez, C. & Brady, L. (1998) *Principles and Practice of Radiation Oncology* (Lippincott–Raven, Philadelphia).
2. Chon, B. H. & Loeffler, J. S. (2002) *Oncologist* **7,** 136–143.
3. Robertson, J., Clarke, D., Pevzner, M. & Matter, R. (1991) *Cancer (Philadelphia)* **68,** 502–508.
4. Fleck, R., McNeese, M., Ellerbroek, N., Hunter, T. & Holmes, F. (1989) *Int. J. Radiat. Oncol. Biol. Phys.* **17,** 829–833.
5. Savitsky, K., Bar-Shira, A., Gilad, S., Rotman, G., Ziv, Y., Vanagaite, L., Tagle, D. A., Smith, S., Uziel, T., Sfez, S., *et al.* (1995) *Science* **268,** 1749–1753.
6. Stewart, G. S., Maser, R. S., Stankovic, T., Bressan, D. A., Kaplan, M. I., Jaspers, N. G., Raams, A., Byrd, P. J., Petrini, J. H. & Taylor, A. M. (1999) *Cell* **99,** 577–587.
7. Varon, R., Vissinga, C., Platzer, M., Cerosaletti, K., Chrzanowska, K., Saar, K., Beckmann, G., Seemanova, E., Cooper, P., Nowak, N., *et al.* (1998) *Cell* **93,** 467–476.
8. Moshous, D., Callebaut, I., de Chasseval, R., Corneo, B., Cavazzana-Calvo, M., Le Deist, F., Tezcan, I., Sanal, O., Bertrand, Y., Philippe, N., *et al.* (2001) *Cell* **105,** 177–186.
9. West, C., Elyan, S., Berry, P., Cowan, R. & Scott, D. (1995) *Int. J. Radiat. Biol.* **68,** 197–203.
10. Hall, E. J., Schiff, P. B., Hanks, G. E., Brenner, D. J., Russo, J., Chen, J., Sawant, S. G. & Pandita, T. K. (1998) *Cancer J. Sci. Am.* **4,** 385–389.
11. Ramsay, J., Birrell, G. & Lavin, M. (1998) *Radiother. Oncol.* **47,** 125–128.
12. Oppitz, U., Bernthaler, U., Schindler, D., Sobeck, A., Hoehn, H., Platzer, M., Rosenthal, A. & Flentje, M. (1999) *Int. J. Radiat. Oncol. Biol. Phys.* **44,** 981–988.
13. Johansen, J., Bentzen, S. M., Overgaard, J. & Overgaard, M. (1996) *Radiother. Oncol.* **40,** 101–109.
14. Russell, N. S., Grummels, A., Hart, A. A., Smolders, I. J., Borger, J., Bartelink, H. & Begg, A. C. (1998) *Int. J. Radiat. Biol.* **73,** 661–670.
15. Peacock, J., Ashton, A., Bliss, J., Bush, C., Eady, J., Jackson, C., Owen, R., Regan, J. & Yarnold, J. (2000) *Radiother. Oncol.* **55,** 173–178.
16. Crompton, N. E., Miralbell, R., Rutz, H. P., Ersoy, F., Sanal, O., Wellmann, D., Bieri, S., Coucke, P. A., Emery, G. C., Shi, Y. Q., Blattmann, H. & Ozsahin, M. (1999) *Int. J. Radiat. Oncol. Biol. Phys.* **45,** 707–714.
17. Barber, J. B., Burrill, W., Spreadborough, A. R., Levine, E., Warren, C., Kiltie, A. E., Roberts, S. A. & Scott, D. (2000) *Radiother. Oncol.* **55,** 179–186.
18. Turesson, I., Nyman, J., Holmberg, E. & Oden, A. (1996) *Int. J. Radiat. Oncol. Biol. Phys.* **36,** 1065–1075.
19. Tusher, V., Tibshirani, R. & Chu, G. (2001) *Proc. Natl. Acad. Sci. USA* **98,** 5116–5121.
20. Tibshirani, R., Hastie, T., Narashimhan, B. & Chu, G. (2002) *Proc. Natl. Acad. Sci. USA* **99,** 6567–6572.
21. Ambroise, C. & McLachlan, G. J. (2002) *Proc. Natl. Acad. Sci. USA* **99,** 6562–6566.
22. Tibshirani, R., Hastie, T., Narasimhan, B. & Chu, G. (2003) *Stat. Sci.* **18,** 104–117.
23. Flickinger, J. C., Kondziolka, D., Lunsford, L. D., Kassam, A., Phuong, L. K., Liscak, R. & Pollock, B. (2000) *Int. J. Radiat. Oncol. Biol. Phys.* **46,** 1143–1148.
24. Eisen, M., Spellman, P., Brown, P. & Botstein, D. (1998) *Proc. Natl. Acad. Sci. USA* **95,** 14863–14868.
25. Tagesson, C., Kallberg, M., Klintenberg, C. & Starkhammar, H. (1995) *Eur. J. Cancer* **31A,** 934–940.
26. Loft, S. & Poulsen, H. E. (1996) *J. Mol. Med.* **74,** 297–312.
27. Erhola, M., Toyokuni, S., Okada, K., Tanaka, T., Hiai, H., Ochi, H., Uchida, K., Osawa, T., Nieminen, M. M., Alho, H. & Kellokumpu-Lehtinen, P. (1997) *FEBS Lett.* **409,** 287–291.
28. Haghdoost, S., Svoboda, P., Naslund, I., Harms-Ringdahl, M., Tilikides, A. & Skog, S. (2001) *Int. J. Radiat. Oncol. Biol. Phys.* **50,** 405–410.
29. West, S. C. & Connolly, B. (1992) *Mol. Microbiol.* **6,** 2755–2759.
30. Akhmedov, A. T. & Lopez, B. S. (2000) *Nucleic Acids Res.* **28,** 3022–3030.
31. Lange-Carter, C. A., Pleiman, C. M., Gardner, A. M., Blumer, K. J. & Johnson, G. L. (1993) *Science* **260,** 315–319.
32. Hanada, M., Ninomiya-Tsuji, J., Komaki, K., Ohnishi, M., Katsura, K., Kanamaru, R., Matsumoto, K. & Tamura, S. (2001) *J. Biol. Chem.* **276,** 5753–5759.
33. Watson, C. A., Chang-Liu, C. M. & Woloschak, G. E. (2000) *Int. J. Radiat. Biol.* **76,** 1455–1461.
34. Gomes-Marcondes, M. C. & Tisdale, M. J. (2002) *Cancer Lett. (Shannon, Irel.)* **180,** 69–74.
35. Delic, J., Morange, M. & Magdelenat, H. (1993) *Mol. Cell. Biol.* **13,** 4875–4883.
36. Badie, C., Itzhaki, J. E., Sullivan, M. J., Carpenter, A. J. & Porter, A. C. (2000) *Mol. Cell. Biol.* **20,** 2358–2366.
37. Fujii, M., Hayashi, K., Niki, M., Chiba, N., Meguro, K., Endo, K., Kameoka, J., Ito, S., Abe, K., Watanabe, T. & Satake, M. (1998) *Oncogene* **17,** 1813–1820.
38. Belzacq, A. S., Vieira, H. L., Kroemer, G. & Brenner, C. (2002) *Biochimie* **84,** 167–176.
39. Brenner, C., Cadiou, H., Vieira, H. L., Zamzami, N., Marzo, I., Xie, Z., Leber, B., Andrews, D., Duclohier, H., Reed, J. C. & Kroemer, G. (2000) *Oncogene* **19,** 329–336.

Downloaded by guest on February 24, 2022